PHYSICAL REVIEW B **85**, 100508(R) (2012)

Unified one-band Hubbard model for magnetic and electronic spectra of the parent compounds of cuprate superconductors

B. Dalla Piazza,[1] M. Mourigal,[1,2] M. Guarise,[3] H. Berger,[3] T. Schmitt,[4] K. J. Zhou,[4] M. Grioni,[3] and H. M. Rønnow[1]

[1]*Laboratory for Quantum Magnetism, École Polytechnique Fédérale de Lausanne (EPFL), CH-1015, Switzerland*

[2]*Institut Laue-Langevin, BP 156, FR-38042 Grenoble Cedex 9, France*

[3]*Laboratory of Photoelectron Spectroscopy, École Polytechnique Fédérale de Lausanne (EPFL), CH-1015, Switzerland*

[4]*Swiss Light Source, Paul Scherrer Institut, CH-5232 Villigen PSI, Switzerland*

(Received 21 April 2011; revised manuscript received 31 October 2011; published 27 March 2012)

Using low-energy projection of the one-band t-t'-t'' Hubbard model we derive an effective spin Hamiltonian and its spin-wave expansion to order $1/S$. We fit the spin-wave dispersion of several parent compounds to the high-temperature superconducting cuprates La_2CuO_4, $Sr_2CuO_2Cl_2$, and $Bi_2Sr_2YCu_2O_8$. Our accurate quantitative determination of the one-band Hubbard model parameters allows prediction and comparison to experimental results. Among those we discuss the two-magnon Raman peak line shape, the K-edge resonant inelastic x-ray scattering 500-meV peak, and the high-energy kink in the angle-resolved photoemission spectroscopy quasiparticle dispersion, also known as the waterfall feature.

DOI: 10.1103/PhysRevB.85.100508 PACS number(s): 74.72.Cj, 74.25.Jb, 75.30.Ds, 78.70.Ck

High-T_c superconductors challenge all known theoretical approaches by mixing charge and magnetic degrees of freedom and by lacking a small variational parameter. The one-band Hubbard model (1bHub), proposed to describe their CuO_2 planes,[1] includes both of these difficulties in its parameters, the electron filling, the hopping matrix element t, and the Coulomb repulsion U. The ratio t/U is moderately small in the cuprates, thus most approaches project out double occupancies (DOs) to obtain the Heisenberg model at half filling or the t-J model for hole or electron doping. Such a projection cannot to be carried out exactly but may be performed as an expansion in powers of t/U.[2]

Experimentally, different techniques have probed separate channels—magnetic or electronic. Inelastic neutron scattering (INS) on La_2CuO_4 (Ref. 3) demonstrated that the projection must be carried out at least to the fourth order (t^4/U^3) to reproduce the observed magnetic excitation spectrum. Angle-resolved photoemission spectroscopy (ARPES) indicates that first-, second-, and third-nearest-neighbor hopping matrix elements are needed to reproduce the Fermi surface and quasiparticle dispersion.[4] A quantitative description of the undoped high-T_c parent compounds therefore needs a model incorporating both of those considerations.[5]

In this Rapid Communication, we develop such a quantitative theory and present the resulting sets of 1bHub parameters for single and bilayer undoped cuprates $Sr_2CuO_2Cl_2$ (SCOC),[6] La_2CuO_4 (LCO),[7] and $Bi_2Sr_2YCu_2O_8$ (BSYCO) (this work), obtained by fitting their magnetic excitation spectra measured by resonant inelastic x-ray scattering (RIXS) and INS.

We start from the 1bHub Hamiltonian

$$\hat{\mathcal{H}} = -\sum_{i,\tau,\sigma} t_\tau c^\dagger_{i,\sigma} c_{i+\tau,\sigma} + U \sum_i n_{i,\uparrow} n_{i,\downarrow}, \qquad (1)$$

where $c^\dagger_{i,\sigma}$ and $c_{i,\sigma}$ creates or destroys a fermion with spin σ on site i, t_{ij} is the hopping matrix element between sites i and j, U is the effective on-site repulsion, and $n_{i,\sigma} = c^\dagger_{i,\sigma} c_{i,\sigma}$. At half filling, the kinetic term mixes states with a different number of DOs, which in the limit $t/U \ll 1$ separate into different energy scales. We use a unitary transformation $\mathcal{H}_{\text{eff}} = e^{iS}\mathcal{H}e^{-iS}$ up to order t^4/U^3 to decouple these states. Following MacDonald *et al.*,[2] we expand Eq. (1) in terms of the operators T^τ_1, T^τ_{-1}, and T^τ_0, respectively creating, destroying, and moving a DO and/or a hole. To fourth order,

$$\hat{\mathcal{H}}^{(4)} = \frac{1}{U}\sum_\tau T^\tau_{-1} T^\tau_1 + \frac{1}{2U^3} \sum_{\substack{\tau_1,\tau_2,\\ \tau_3,\tau_4}} 2T^{\tau_1}_{-1} T^{\tau_2}_1 T^{\tau_3}_{-1} T^{\tau_4}_1 - T^{\tau_1}_{-1} T^{\tau_2}_{-1} T^{\tau_3}_1 T^{\tau_4}_1 - T^{\tau_1}_{-1} T^{\tau_2}_0 T^{\tau_3}_0 T^{\tau_4}_1 + O\left(\frac{1}{U^4}\right). \qquad (2)$$

The effective spin Hamiltonian is then calculated from the matrix elements $\langle\alpha|\hat{\mathcal{H}}^{(m)}|\beta\rangle$, where $|\alpha\rangle$ and $|\beta\rangle$ are singly occupied spin states. In the subspace with no DO, the $T^{\tau_1}_{-1} T^{\tau_2}_0 T^{\tau_3}_0 T^{\tau_4}_1$ matrix elements can only be finite if τ_1, τ_2, τ_3, and τ_4 form a closed loop as the DO and the hole must meet to annihilate (Fig. 1, top). Apart from four-hop loops, $T^{\tau_1}_{-1} T^{\tau_2}_1 T^{\tau_3}_{-1} T^{\tau_4}_1$ and $T^{\tau_1}_{-1} T^{\tau_2}_{-1} T^{\tau_3}_1 T^{\tau_4}_1$ may also contribute on disjoint bonds τ and τ', but in this case the two operator contributions get canceled out since $[T^\tau_m, T^{\tau'}_{m'}] = 0$. Therefore the effective Hamiltonian can be written as a sum over loop ensembles:[8]

$$\hat{\mathcal{H}}^{(4)} = \sum_{\{\,\}} \left(\frac{4t^2_{12}}{U} - \frac{16t^4_{12}}{U^3}\right)\mathbf{S}_1\mathbf{S}_2 + \sum_{\{\,\}} \frac{4t^2_{12}t^2_{23}}{U^3}\mathbf{S}_1\mathbf{S}_3 - \sum_{\{\,\}} \frac{4t_{12}t_{23}t_{34}t_{41}}{U^3}\left\{\sum_{\substack{i,j=1\\ i\neq j}}^{4} \mathbf{S}_i\mathbf{S}_j - 20[(\mathbf{S}_1\mathbf{S}_2)(\mathbf{S}_3\mathbf{S}_4) + (\mathbf{S}_1\mathbf{S}_4)(\mathbf{S}_2\mathbf{S}_3) - (\mathbf{S}_1\mathbf{S}_3)(\mathbf{S}_2\mathbf{S}_4)]\right\} + E^{(4)}, \qquad (3)$$

where $E^{(4)}$ is a constant and $\{\,\}$, $\{\,\}$, and $\{\,\}$ stand for the ensembles of two, three, and four sites connected as sketched. We emphasize that the plaquette ensembles are fully defined by the considered hopping matrix elements

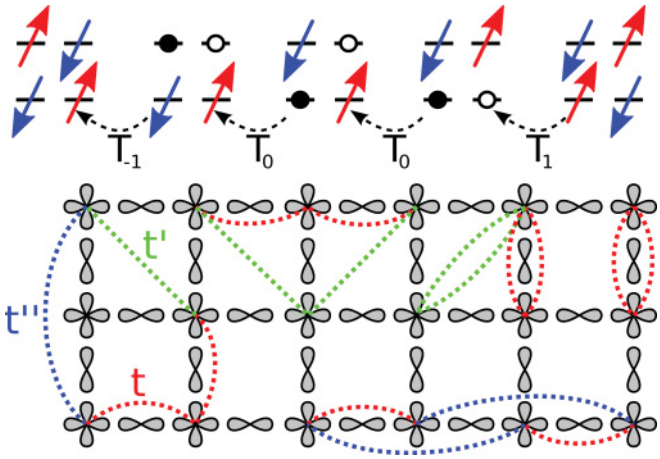

FIG. 1. (Color online) Top: Example of an exchange process contributing to the matrix element $\langle \begin{smallmatrix}\uparrow & \downarrow \\ \downarrow & \uparrow\end{smallmatrix} | T_{-1}T_0T_0T_1 | \begin{smallmatrix}\downarrow & \uparrow \\ \uparrow & \downarrow\end{smallmatrix} \rangle$. Plain (open) points are DOs (holes). Bottom: CuO_2 planes from the perovskite structure. Examples of exchange loops from the effective spin Hamiltonian of Eq. (3) are indicated with first-, second-, and third-nearest-neighbor hoppings t, t', and t''.

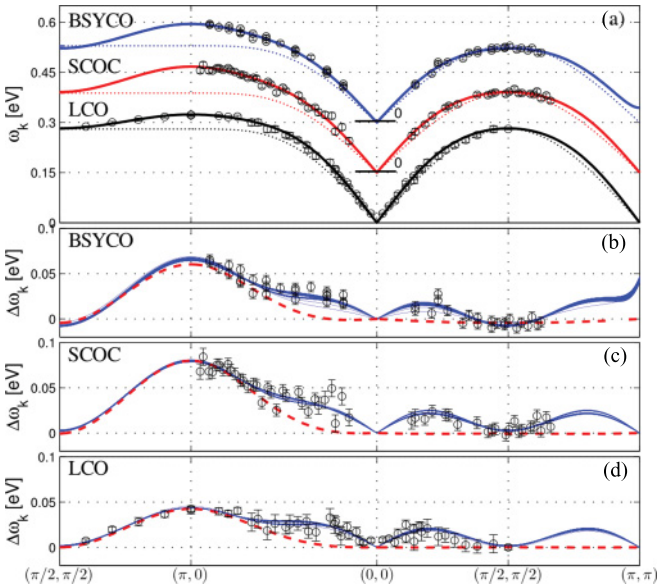

FIG. 2. (Color online) (a) Fits of the measured SW dispersions (solid lines) and the 1JHei SW dispersion (dotted lines) with $J_{NN} = \omega_{(\pi/2,\pi/2)}/2Z_c$. From top to bottom: BSYCO ($J_{NN} = 0.15$ eV), SCOC (Ref. 6) ($J_{NN} = 0.12$ eV), and LCO (Ref. 7) ($J_{NN} = 0.14$ eV). (b)–(d) Same as in (a) but subtracted from the 1JHei SW dispersion to enhance details. Dashed lines are the SW dispersions obtained from the Hubbard model with only NN hopping t. Data points from experiments are folded onto the equivalent high-symmetry axes of the first Brillouin zone.

t_τ and the lattice topology, so that Eq. (3) is the general low-energy projection to order t^4/U^3 of the 1bHub at half filling for any lattice. Examples of plaquettes of two, three, and four sites involving first-, second-, and third-nearest-neighbor (NN) hopping amplitudes t, t', and t'' are sketched on the bottom of Fig. 1. The four-spin exchange term has been derived in the past for NN hopping alone[2,9] and is important for the magnetism of a large variety of systems.[10–15] Here we generalize this result for an arbitrary set of hopping amplitudes. A similar development but away from half filling would result in a t-J model with the same magnetic couplings as in Eq. (3) plus a family of charge plaquette hoppings.

The derivation of measurable quantities is easier for the insulating parent compounds. Here, we use spin-wave (SW) theory to derive the dispersion of magnetic excitations. We expand the spin operators of Eq. (3) in terms of Holstein-Primakov bosons around the classical antiferromagnetic ground state (GS). Keeping the first $1/S$ correction for the t_τ^2/U terms, the Hamiltonian transforms as $\hat{\mathcal{H}}^{(4)} = E_N + \hat{\mathcal{H}}_2 + \hat{\mathcal{H}}_4 + O(1/S)$, where the Néel GS energy E_N includes the constant of Eq. (3), and the harmonic dispersion $\omega_0(\mathbf{k})$ is obtained from a Bogoliubov transform of the quadratic term $\hat{\mathcal{H}}_2$. A Hartree-Fock decoupling[16] of the quartic term $\hat{\mathcal{H}}_4$ results in an overall momentum-dependent correction to the magnon energy, so that our final SW Hamiltonian reads

$$\hat{\mathcal{H}}^{(4)} = \sum_{\mathbf{k}} Z_c(\mathbf{k})\omega_0(\mathbf{k})\alpha_{\mathbf{k}}^\dagger\alpha_{\mathbf{k}} + E_N + \delta E, \qquad (4)$$

where α's are free magnon operators, $Z_c(\mathbf{k})$ is the $1/S$ renormalization of their dispersion, and δE is the quantum correction to the GS energy at this order. Compared to the bare NN Heisenberg model (1JHeis), the inclusion of the ring exchange terms qualitatively alter the SW mode, resulting in a magnetic zone boundary (ZB) dispersion and a greater SW velocity. For the bilayer square lattice, Eq. (3) is still valid but the plaquette ensembles now include interlayer hopping $t_\perp$, and two boson flavors to account for the top and bottom sites. This results in two magnon modes gapped respectively at $(0,0)$ and (π,π) but degenerate along the ZB.

Before applying the result to the cuprate compounds SCOC (Ref. 6) and LCO,[7] we report here measurements of the SW dispersion in $Bi_2Sr_2YCu_2O_8$, a bilayer parent compound. Single crystals were grown by the flux method, with yttrium ensuring an insulating antiferromagnetic phase. The SW dispersion was measured using Cu L_3 edge RIXS at the Super Advanced X-ray Spectrometer (SAXES) end station of the Swiss Light Source Advanced Resonant Spectroscopies (ADRESS) beamline, with experimental details and data analysis as described previously.[6]

The SW dispersion of each compound is shown in Fig. 2. They all feature a dispersion between the ZB points $(\pi,0)$ and $(\pi/2,\pi/2)$ which can in principle be explained by the effective model of Eq. (3) with NN hopping alone [Figs. 2(b)–2(d), dashed lines]. However, this approach results in unphysically low $U = 2.2$ eV (Ref. 3) for LCO and $U < 2$ eV for SCOC and BSYCO. Although U is an effective on-site repulsion, closer to the charge-transfer (CT) gap than to the bare Coulomb repulsion, a good 1bHub must use an effective parameter compatible with electronic and optical spectroscopies, which request $U \sim 3$–4 eV for the cuprates.[17] We therefore include second- and third-NN hopping in our fit, which now has four parameters (U,t,t',t''). The measured SW dispersions contain three distinct constraints, the $(\pi,0)$ and $(\pi/2,\pi/2)$ ZB energies and the SW velocity. We thus expect a one-dimensional solution and choose the free parameter to be U. The fitting procedure is as follows. For a fixed choice of $(U,t''/t)$ we fit

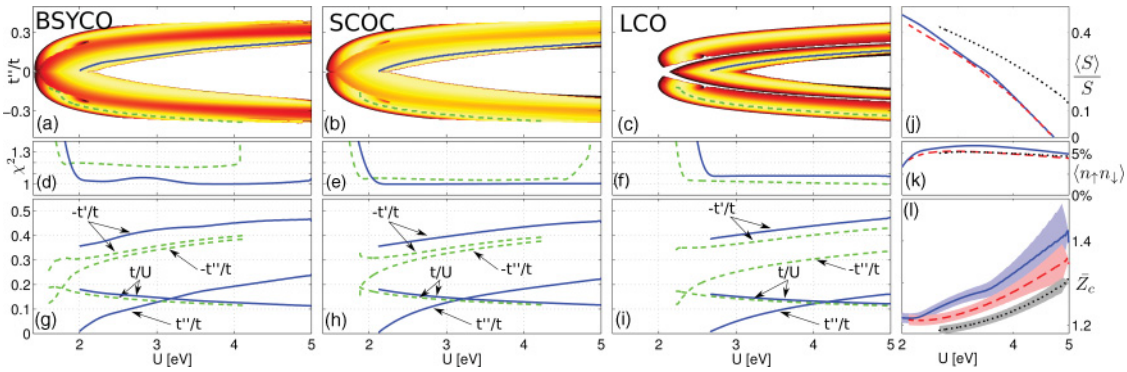

FIG. 3. (Color online) Summary of the fitting results. (a)–(c) Goodness (χ^2) of the $(t/U,t'/t)$ fit for fixed $(U,t''/t)$. Solid (blue) and dashed (green) lines are best-fit solutions as functions of U for $t't'' < 0$ and $t't'' > 0$, respectively. (d)–(f) χ^2 along the best-fit lines defined in (a)–(c). (g)–(i) $(t/U,t'/t,t''/t)$ solutions along the best-fit lines defined in (a)–(c). (j)–(l) Staggered magnetization, DO density, and **k**-averaged quantum $1/S$ renormalization Z_c along the $t't'' < 0$ best-fit lines defined in (a)–(d). Lines: Solid blue BSYCO, dashed red SCOC, and dotted black LCO. Shaded areas indicate **k** variation of Z_c.

the two other parameters t/U and t'/t. As the calculation of the $1/S$ estimate of Z_c involves a slowly convergent integration over **k** space, we include it in a two-step iterative approach. First, we fix it to the uniform $Z_0 = 1.1579$ obtained for the 1JHei. Then we fit $Z_0\omega_{\mathbf{k}}(U,t,t',t'')$ and calculate a first nonuniform $Z_1(\mathbf{k})$ from the obtained parameter set. We iterate this procedure until $Z_n(\mathbf{k})$ converges, typically after 10–15 steps. In the case of BSYCO, we further include an interplane hopping $t_\perp$. However, the resolution of RIXS does not allow to distinguish the splitting of the two magnon modes, thus we fix $t_\perp = 54$ meV as reported by Chuang *et al.*[18]

The fitting results over the $(U,t''/t)$ plane are shown in Fig. 3 with the $(t/U,t'/t,t''/t)$ parameters along the best-fit lines. Overall, the three compounds share common features, i.e., a strong lower boundary for U, an increase of $|t'|/t$ and t''/t with U, and a slowly varying t/U. Due to the $t^2t't''/U^3$ term, the calculated magnon dispersion is symmetric in the signs of t and t' but not in the relative sign of t' and t'', resulting in two separate solutions for $t't'' < 0$ and $t't'' > 0$. From the best-fit lines, one can see that the inclusion of $|t''|$ is necessary in order to get $U \approx 3$–4 eV. For some regions of the $(U,t''/t)$ space, the Néel state is not the classical GS of Eq. (3), and/or is destroyed by quantum fluctuations. Both cases can be systematically determined by looking at the size of zero-point fluctuations $\langle a_i^\dagger a_i \rangle$. The outermost void regions in Figs. 3(a)–3(c) are those where Néel order is unstable. In Fig. 3(j), we show the effective staggered magnetization $\tilde{M}_{\text{alt}} = e^{iS} M_{\text{alt}} e^{-iS} \simeq (1 - 8\frac{t^2}{U^2}) M_{\text{alt}}$ (Ref. 5) as a function of U along the best-fit lines. By increasing U, t' and t'' grow while t/U stays roughly constant, bringing more frustration and subsequently reducing the ordered moment. We calculate the DO density using the Feynman-Hellmann theorem $\langle n_{i,\uparrow} n_{i,\downarrow} \rangle = \partial \langle \hat{\mathcal{H}}^{(4)} \rangle / \partial U$. Along the best-fit lines, a U-independent value of 5% is found for all cuprates, in agreement with the electronic shielding factor calculated in Ref. 19. The $1/S$ estimate of $Z_c(\mathbf{k})$ is found to vary by only about 2% across the Brillouin zone. It thus mainly affects the overall energy scale dominated by $\frac{t^2}{U}$. For a given U, it decreases the value of t, keeping t'/t and t''/t unchanged. Further magnon-magnon interactions have been shown to bring small corrections to $Z_c(\mathbf{k})$ (Ref. 20) in the case of 1JHeis. We expect this still is the case in our model. In Fig. 3(l) we show the average value, which varies from 1.2 to 1.3 for $U \approx 3$–4 eV, which again reveals the prominent role of quantum fluctuations in the range of parameters relevant for the cuprates.

The effective U cannot be directly obtained through magnetic excitations. However, more direct experimental techniques may give good estimates of U, thus determining a unique set of 1bHub parameters for each of the above compounds. In particular, an estimate of the 1bHub parameters of SCOC was obtained from ARPES (Ref. 17) as $U = 3.5$ eV, $t = 0.35$ eV, $t' = -0.12$ eV, and $t'' = 0.08$ eV. Consistently with those parameters and in order to compare the three cuprate compounds, in Table I we adopt a uniform value of $U = 3.5$ eV and the $t't'' < 0$ solution. A more accurate determination of U could be found in the CT excitation part of the RIXS spectrum. Using the above ARPES parameter estimates, Hasan *et al.* could identify a dispersing excitation around 3 eV in Cu K-edge RIXS as CT excitation.[21] A similar approach using our parameter sets would allow unambiguous determination of U.

Having established a quantitative model allows to predict further quantities. We compute the noninteracting two-magnon (2M) density of states (DOS) underlying, at (0,0), Raman scattering and, at $(\pi,0)$, K-edge RIXS, and the 2M dynamical structure factor $S^{zz}(\mathbf{k},\omega)$ probed by INS. For $S^{zz}(\mathbf{k},\omega)$ we omit the t^2/U^2 corrections coming from the unitary transformation. Although a higher-order magnon interaction affects those 2M quantities,[22–24] our results already allow several observations. Compared to 1JHei, our predictions show the enhancement of a 500-meV peak in S^{zz} at $(\pi,0)$ [Fig. 4(d)], which shows that attempts to explain the reported INS line shape at $(\pi,0)$ from

TABLE I. Parameters determined from the SW fits with fixed $U = 3.5$ eV and $t't'' < 0$.

	t (meV)	t' (meV)	t'' (meV)	$\langle S \rangle / S$	c (meVÅ)	$\langle n_{i,\uparrow} n_{i,\downarrow} \rangle$
BSYCO	470(10)	−205(3)	79(4)	0.3	0.146	5.9%
SCOC	480(10)	−200(5)	75(5)	0.29	0.163	5.1%
LCO	492(7)	−207(3)	45(2)	0.4	0.195	5.2%

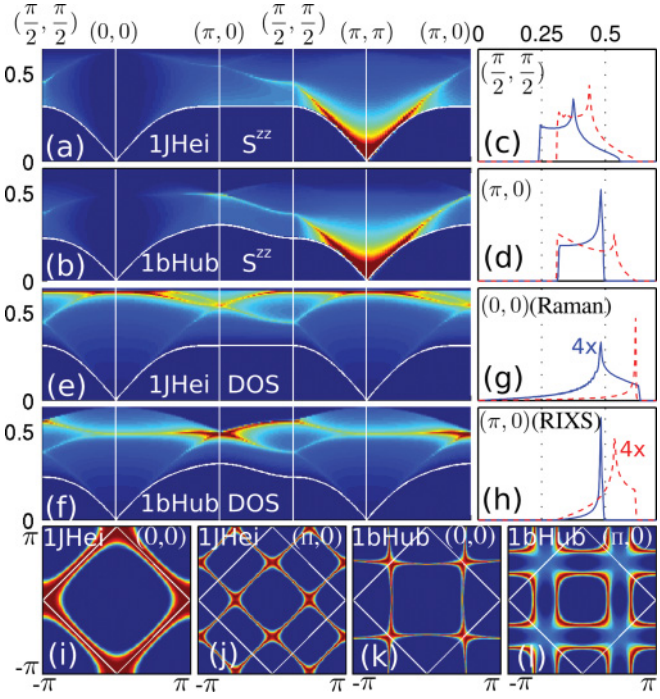

FIG. 4. (Color online) (a), (b) $S^{zz}(\mathbf{k},\omega)$ for 1JHei with $J_{\rm NN} = \omega_{(\pi,0)}/2Z_c$ and the 1bHub with the SCOC parameters. (c), (d) S^{zz} energy line shapes at the ZB points for 1JHei (dashed red line) and 1bHub (solid blue line). (e), (f) Corresponding 2M DOS. (g), (h) DOS profiles at (0,0) and $(\pi,0)$. (i), (j) Single-magnon wave vectors contributing to the DOS peaks at (0,0) and $(\pi,0)$ in 1JHei and (k), (l) in the SCOC 1bHub.

quantum effects must consider the full Hamiltonian presented here.[7,25,26] Also, along the ZB, the intensity of the one-magnon (transverse) excitations is constant, so that the missing SW amplitude observed by INS (Refs. 7,25,27, and 28) *does not* result from further neighbor hopping.

In the 1JHei, the (0,0) 2M DOS peaks at $4Z_cJ_{\rm NN}$, corresponding to creating two spin waves at the ZB. The peak in Raman B_{1g} spectra is found at 0.37 eV for SCOC (Ref. 29) corresponding to $\sim 2.8J_{\rm NN}$. The reduced energy was explained as due to magnon-magnon interactions,[23] but the peak width could not be reproduced. The large ZB dispersion that our model entails first implies that experiments should not be compared to a single $J_{\rm NN}$. Second, it explains the Raman peak width as a range of energies from $2\omega_{(\pi,0)}$ extending down to $2\omega_{(\frac{\pi}{2},\frac{\pi}{2})}$, where a maximum occurs because at this energy entire lines in one-magnon momentum space contribute [Fig. 4(k)]. Third, it predicts a lower peak energy requiring weaker magnon interactions to match experiments. For a correct calculation of magnon interactions, we caution that, in the cuprates, it is a different one-magnon interaction that contributes to the Raman peak [Fig. 4(k)] than in the 1JHei [Fig. 4(i)]. The observation of a strong excitation at $(\pi,0)$ in K-edge RIXS (Ref. 30) is also explained by our calculations, which demonstrate a concentration of DOS at exactly this wave vector. Again the one-magnon states that contribute to this peak [Fig. 4(l)] are very different from the 1JHei [Fig. 4(j)]. Thus, our results reveal dramatic differences in the 2M continuum, implying that INS, L_3, or K-edge RIXS and Raman data must be interpreted using the full quantitative model derived here.

Our model also provides insight into the electronic spectra, such as the quasiparticle dispersion measured by ARPES. It has been debated whether a universal kink for undoped and doped cuprates discovered around 0.4 eV (Refs. 31 and 32) (the waterfall feature) should be interpreted as (i) a shallow dispersion with $t = 0.23$ eV,[33] followed by a strong ARPES matrix element effect[34] above 0.4 eV, or as (ii) a self-energy kink on a stronger dispersing bare band ($t = 0.48$ eV).[35] Our results for LCO ($t = 0.49$ eV) thus provide strong support for the second scenario, hence evidence of a strong quasiparticle interaction, which in turn could be important for the mechanism of high-T_c superconductivity.

In summary, we derived an effective spin Hamiltonian that is valid for any lattice and any hopping matrix element range. Using SW theory with $1/S$ corrections and three hoppings t, t', and t'', we obtain accurate 1bHub parameter sets for several parent compounds of the cuprate superconductors. We predict an ordered moment, DO density, SW renormalization, and 2M spectra. From the noninteracting 2M $S^{zz}(\boldsymbol{q},\omega)$ and DOS, we clearly demonstrate the necessity to include the extended exchange paths to interpret Raman and K-edge RIXS peaks. Furthermore, electronic spectra such as ARPES could also be addressed using the same 1bHub parameters.

We gratefully acknowledge N. S. Headings *et al.* for sharing their data, J. Chang, F. Vernay, F. Mila, T. A. Tóth, B. Normand, and M. E. Zhitomirsky for fruitful discussions, and the Swiss NSF and the MaNEP NCCR for support.vv

[1] P. W. Anderson, Science **235**, 1196 (1987).
[2] A. H. MacDonald, S. M. Girvin, and D. Yoshioka, Phys. Rev. B **37**, 9753 (1988).
[3] R. Coldea, S. M. Hayden, G. Aeppli, T. G. Perring, C. D. Frost, T. E. Mason, S. W. Cheong, and Z. Fisk, Phys. Rev. Lett. **86**, 5377 (2001).
[4] A. Damascelli, Z. Hussain, and Z.-X. Shen, Rev. Mod. Phys. **75**, 473 (2003).
[5] J. Y. P. Delannoy, M. J. P. Gingras, P. C. W. Holdsworth, and A. M. S. Tremblay, Phys. Rev. B **79**, 235130 (2009).
[6] M. Guarise, B. Dalla Piazza, M. Moretti Sala, G. Ghiringhelli, L. Braicovich, H. Berger, J. N. Hancock, D. van der Marel, T. Schmitt, V. N. Strocov, L. J. P. Ament, J. van den Brink, P.-H. Lin, P. Xu, H. M. Rønnow, and M. Grioni, Phys. Rev. Lett. **105**, 157006 (2010).
[7] N. S. Headings, S. M. Hayden, R. Coldea, and T. G. Perring, Phys. Rev. Lett. **105**, 247001 (2010).
[8] See Supplemental Material at http://link.aps.org/supplemental/10.1103/PhysRevB.85.100508 for the closed loops demonstration.
[9] M. Takahashi, J. Phys. C **10**, 1289 (1977).
[10] A. Läuchli, J. C. Domenge, C. Lhuillier, P. Sindzingre, and M. Troyer, Phys. Rev. Lett. **95**, 137206 (2005).
[11] A. Chubukov, E. Gagliano, and C. Balseiro, Phys. Rev. B **45**, 7889 (1992).

[12]D. J. Thouless, Proc. Phys. Soc. **86**, 893 (1965).
[13]M. Roger, J. H. Hetherington, and J. M. Delrieu, Rev. Mod. Phys. **55**, 1 (1983).
[14]G. Misguich, B. Bernu, C. Lhuillier, and C. Waldtmann, Phys. Rev. Lett. **81**, 1098 (1998).
[15]M. Katano and D. S. Hirashima, Phys. Rev. B **62**, 2573 (2000).
[16]T. Oguchi, Phys. Rev. **117**, 117 (1960).
[17]T. Tohyama and S. Maekawa, Supercond. Sci. Technol. **13**, R17 (2000).
[18]Y.-D. Chuang, A. D. Gromko, A. V. Fedorov, Y. Aiura, K. Oka, Y. Ando, M. Lindroos, R. S. Markiewicz, A. Bansil, and D. S. Dessau, Phys. Rev. B **69**, 094515 (2004).
[19]J. Lorenzana, G. Seibold, and R. Coldea, Phys. Rev. B **72**, 224511 (2005).
[20]J. I. Igarashi, Phys. Rev. B **46**, 10763 (1992).
[21]M. Z. Hasan, E. D. Isaacs, Z.-X. Shen, L. L. Miller, K. Tsutsui, T. Tohyama, and S. Maekawa, Science **288**, 1811 (2000).
[22]C. M. Canali and M. Wallin, Phys. Rev. B **48**, 3264 (1993).
[23]C. M. Canali and S. M. Girvin, Phys. Rev. B **45**, 7127 (1992).
[24]T. Nagao and J. I. Igarashi, Phys. Rev. B **75**, 214414 (2007).
[25]N. B. Christensen, H. M. Rønnow, D. F. McMorrow, A. Harrison, T. G. Perring, M. Enderle, R. Coldea, L. P. Regnault, and G. Aeppli, Proc. Natl. Acad. Sci. USA **104**, 15264 (2007).
[26]N. Tsyrulin, F. Xiao, A. Schneidewind, P. Link, H. M. Rønnow, J. Gavilano, C. P. Landee, M. M. Turnbull, and M. Kenzelmann, Phys. Rev. B **81**, 134409 (2010).
[27]H. M. Rønnow, D. F. McMorrow, R. Coldea, A. Harrison, I. D. Youngson, T. G. Perring, G. Aeppli, O. Syljuasen, K. Lefmann, and C. Rischel, Phys. Rev. Lett. **87**, 037202 (2001).
[28]N. B. Christensen, D. F. McMorrow, H. M. Rønnow, A. Harrison, T. G. Perring, and R. Coldea, J. Magn. Magn. Mater. **272**, 896 (2004).
[29]G. Blumberg, P. Abbamonte, M. V. Klein, W. C. Lee, D. M. Ginsberg, L. L. Miller, and A. Zibold, Phys. Rev. B **53**, R11930 (1996).
[30]D. S. Ellis, J. Kim, J. P. Hill, S. Wakimoto, R. J. Birgeneau, Y. Shvyd'ko, D. Casa, T. Gog, K. Ishii, K. Ikeuchi, A. Paramekanti, and Y.-J. Kim, Phys. Rev. B **81**, 085124 (2010).
[31]F. Ronning, K. M. Shen, N. P. Armitage, A. Damascelli, D. H. Lu, Z. X. Shen, L. L. Miller, and C. Kim, Phys. Rev. B **71**, 094518 (2005).
[32]J. Graf, G.-H. Gweon, K. McElroy, S. Y. Zhou, C. Jozwiak, E. Rotenberg, A. Bill, T. Sasagawa, H. Eisaki, S. Uchida, H. Takagi, D.-H. Lee, and A. Lanzara, Phys. Rev. Lett. **98**, 067004 (2007).
[33]A. A. Kordyuk, S. V. Borisenko, A. Koitzsch, J. Fink, M. Knupfer, and H. Berger, Phys. Rev. B **71**, 214513 (2005).
[34]D. S. Inosov, J. Fink, A. A. Kordyuk, S. V. Borisenko, V. B. Zabolotnyy, R. Schuster, M. Knupfer, B. Büchner, R. Follath, H. A. Dürr, W. Eberhardt, V. Hinkov, B. Keimer, and H. Berger, Phys. Rev. Lett. **99**, 237002 (2007).
[35]J. Chang, M. Shi, S. Pailhés, M. Månsson, T. Claesson, O. Tjernberg, A. Bendounan, Y. Sassa, L. Patthey, N. Momono, M. Oda, M. Ido, S. Guerrero, C. Mudry, and J. Mesot, Phys. Rev. B **78**, 205103 (2008).